Ethanol/water mixture permeation through a Nafion®based membrane electrode assembly

S. Kontou, V. Stergiopoulos, S. Song [1], P. Tsiakaras *

Department of Mechanical Engineering, School of Engineering, University of Thessaly, Pedion Areos, 38 334 Volos, Greece

Abstract

In the present work, the permeation behavior of ethanol/water mixtures through a Nafion®-115 based membrane electrode assembly (MEA) has been investigated. The crossover measurements were carried out in a single fuel cell test apparatus. Ethanol aqueous solutions at different concentrations were supplied to the anode compartment while high-purity dry helium was fed to the cathode in order to sweep off the permeated water and ethanol. The quantitative analysis of water and ethanol from the cathode effluent has been carried out on-line by a GC under the following operation conditions: $T_{cell} = 30$–$90\,^{\circ}C$, ethanol aqueous solution concentration $C_{ethanol} = 0$–$12.0\,mol\,L^{-1}$, helium flow rate at the cathode F_{He} in the range of 80–1500 mL min^{-1} and liquid solution flow rate to the anode $F_1 = 0.2\,mL\,min^{-1}$.

It was found that the water crossover rate is almost one order of magnitude higher than ethanol's. It was also found that the ethanol crossover rate depends on ethanol concentration and presents a volcano behavior, with the peak value at ethanol concentration of $8.0\,mol\,L^{-1}$. This could be attributed to the different swelling behavior of the Nafion® membrane in the presence of various ethanol aqueous solutions. A similar behavior was also observed in the case of water with the peak value at $2.0\,mol\,L^{-1}$ which could be attributed to thermodynamical reasons.

1. Introduction

Direct ethanol fuel cells (DEFCs) are considered as the most promising systems for the conversion of chemical energy to electricity due to a number of advantages of ethanol [1,2]. Compared to hydrogen and methanol, which are the most widely investigated fuels for proton exchange membrane fuel cells (PEMFCs), ethanol presents a series of advantages as follows: it is easier than hydrogen to handle, transport, store and distribute, due to the fact that it is liquid, while with respect to methanol it has higher energy density and is non-toxic. Moreover, ethanol oxidation produces only the products that are required by nature to recompose ethanol molecules through the photosynthesis process. Therefore, the net carbon dioxide contribution to the environment is negligible [2].

One of the most critical barriers to improve the DEFC performance is the ability of ethanol to pass through the membrane, from the anode to the cathode side, which is widely known as ethanol crossover. This phenomenon can lead to a mixed potential at the cathode, caused by the simultaneous reactions of ethanol electrooxidation and oxygen reduction, and in this way decreasing the fuel utilization coefficient as well as the fuel cell efficiency [3]. Furthermore, ethanol itself and also its intermediate products can also be adsorbed on the cathode catalyst surface, thus hindering the adsorption of oxygen molecules and consequently decreasing the oxygen reduction rate. Song et al. [3] have already reported ethanol crossover behavior and have compared it with methanol's [4]. They have also investigated the effect of the MEA preparation procedure on both ethanol crossover and DEFC performance [4,5]. Nevertheless, up to date there is not a systematic study for the ethanol and water crossover through the fuel cell's membrane electrode assembly.

One of the other most critical parameters is the water management. In the case of insufficient hydration, the electrolyte membrane will loose its ionic conductivity, which is strongly dependent on the water content in a more or less linear way. On

* Corresponding author. Tel.: +30 24210 74065; fax: +30 24210 74050.
E-mail address: tsiak@mie.uth.gr (P. Tsiakaras).
[1] Present address: State Key Laboratory of Optoelectronic Materials and Technologies, School of Physics and Engineering, Sun Yat-Sen University, Guangzhou 510275, China

the other hand, in the case of excess water, electrode "flooding" can occur, which inevitably covers the catalysts' active sites, and consequently deteriorates the cell performance [6,8]. The water transportation is also related to the current and the characteristics of both the membrane and the electrode. The two main reasons that cause the movement of water molecules through the membrane are the electro osmotic drag, which is caused by the electrical potential gradient and diffusion, which is coming from the existence of water concentration and pressure gradient between the two sides of the membrane [7–10]. However, the crossover mechanism of both water and the fuel (in the present work, ethanol) affects other properties of the membrane as well. Affoune et al. [11] have reported that the membrane's conductivity in aqueous solutions of different alcohols decreases as the alcohol concentration increases. Moreover, the structure of the membrane also changes in high alcohol concentrations, affecting the adsorption of species onto the membrane. Therefore, it is important to detect the optimal feed mixture composition, at which the fuel crossover to the cathode is minimum, while the protonic conductivity remains at an acceptable level.

In the present work, the permeation behavior of ethanol/water mixtures through a Nafion®-115 based MEA was investigated and the effect of the main affecting parameters on both ethanol and water crossover rates was examined.

2. Experimental

2.1. Membrane electrode assembly preparation

A membrane electrode assembly (MEA) was prepared using the conventional method, which has been described previously [2]. Nafion®-115 membrane was used as electrolyte and it was pre-treated by slight boiling in 3–5 wt.% H_2O_2, deionized water, 1.0 mol L^{-1} H_2SO_4 and again in deionised water, for 1 h in each step. Pt/C (40 wt.%, Johnson Matthey Corp.) with a metal loading equal to 2.0 and 1.0 mg cm^{-2} was used as the anode and cathode catalysts, respectively. The catalyst inks were obtained by adding 5% Nafion® solution in the case of the anode and 10% PTFE solution in the cathode case. The as-prepared catalyst inks were brushed onto the corresponding diffusion layer of the electrodes. Then the cathode was treated at 340 °C for 1 h in the inert atmosphere in order to remove the surfactants. After spraying with ca. 0.5 mg cm^{-2} Nafion® solution onto the surface of both anode and cathode, the MEA was obtained by hot pressing both electrodes onto each side of the Nafion®-115 membrane at 140 °C under a pressure of 100 kg cm^{-2}. The geometric area of the MEA was 2.0 cm × 2.0 cm.

2.2. Crossover measurements

Ethanol and water crossover measurements were performed in a single fuel cell test station shown in Fig. 1. The device was heated to the desired temperature by using an electrical heater placed in the middle of the stainless steel bipolar plates and the temperature was monitored by a thermocouple. Ethanol aqueous solutions at different concentrations were supplied to the anode compartment of the cell at a flow rate of 0.2 mL min^{-1} by a syringe pump (KD Scientific). High-purity dry helium streams, controlled by digital mass flow controllers (Brooks 5000), was fed to the cathode at atmospheric pressure and at different flow rates in order to sweep off the permeated ethanol and water. The mechanism of ethanol permeation behavior through the MEA has been described elsewhere [12]. The pressure was stable and equal to 1.0 atm and no current was applied or drawn out during the experiments. The effluent from the cathode was vaporized by a heating line and then analyzed on-line by a TCD gas chromatograph (SHIMADZU GC-14B) equipped with a packed Porapak Q column.
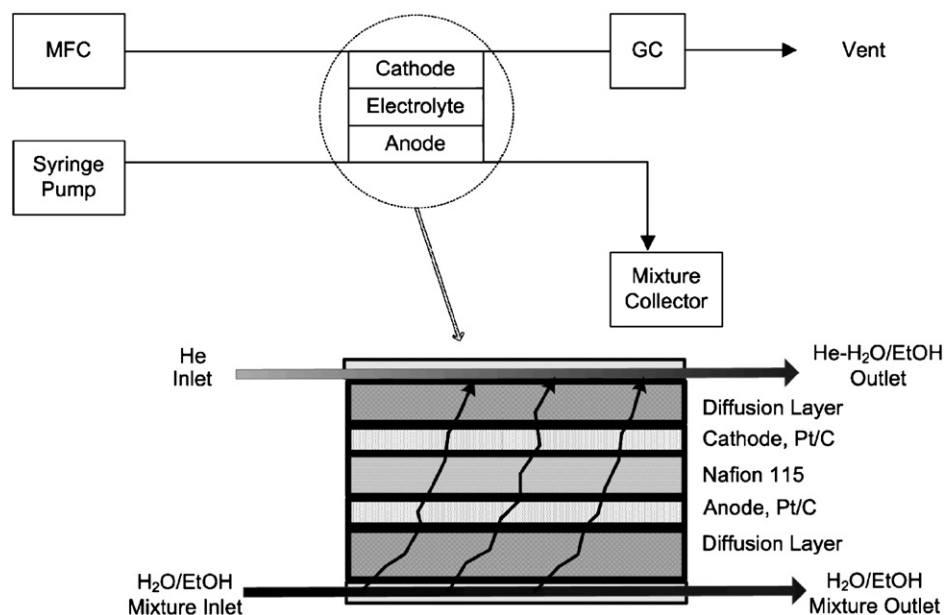

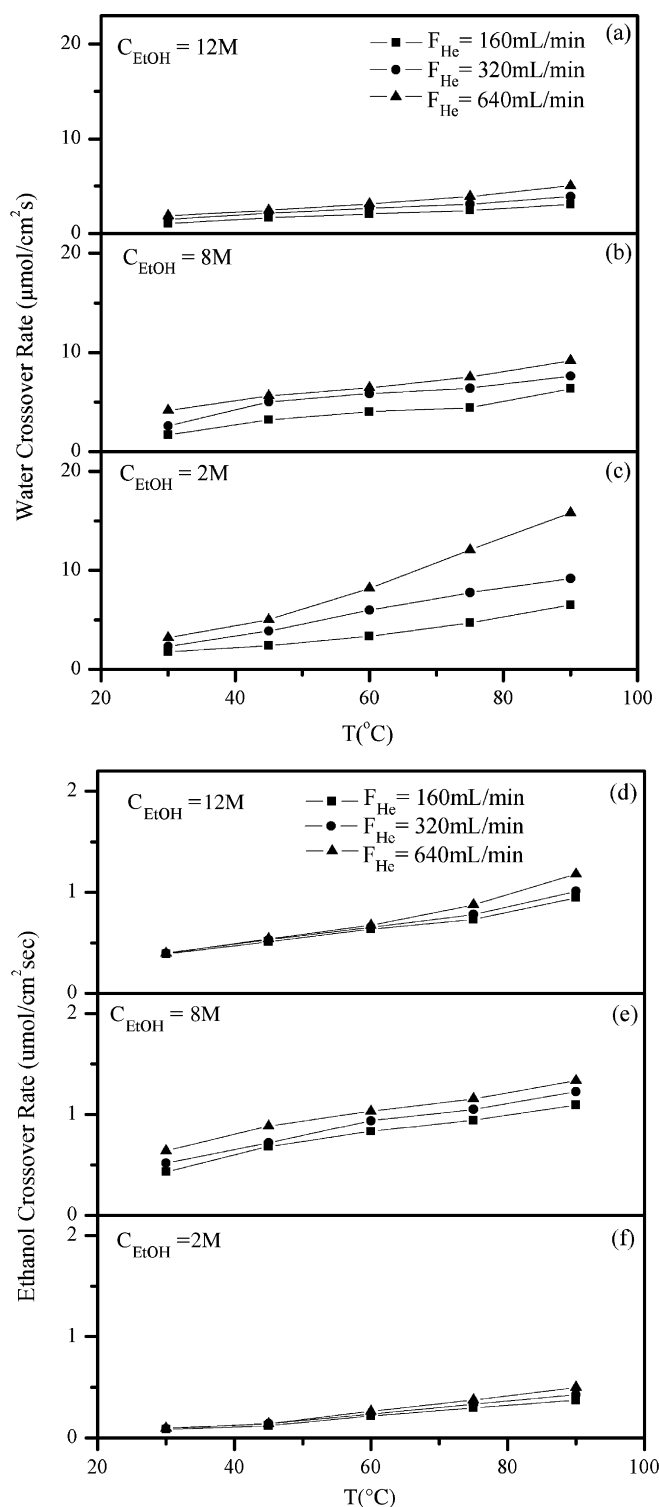
Fig. 1. Fuel cell test apparatus.

Fig. 2. The effect of temperature at different flow rates (a–c) on the water and (d–f) ethanol crossover rate. Anode liquid flow = 0.2 mL min^{-1}, P_{total} = 1 atm and electrode area = 4.0 cm^2.

Fig. 3. Arrhenius plots at flow rate equal to 640 mL min^{-1}. Ethanol concentration: 2.0 and 4.0 mol L^{-1}. Anode liquid flow = 0.2 mL min^{-1}, P_{total} = 1 atm and electrode area = 4 cm^2. The close symbols (●), (■) are referred to water and the open (○), (□) at ethanol.

3. Results and discussion

3.1. The effect of temperature

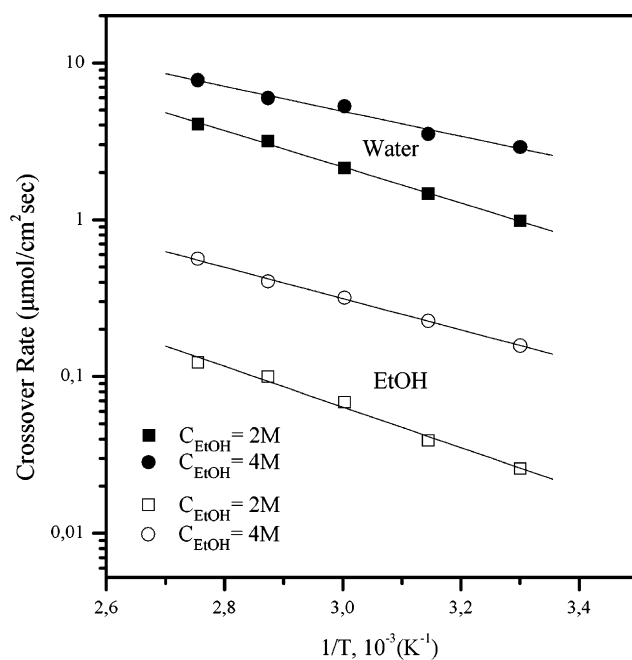Fig. 2 shows the ethanol and water crossover rate at different temperatures. It is obvious that by increasing the cell operation temperature, both water and ethanol crossover rates increase. This could be attributed to the fact that both water and ethanol vapor saturation pressures in the cathode increase sharply with temperature increment, promoting the water and ethanol removal from the cathode carrier (He) [13]. At the same time, the enhanced temperature can accelerate the thermodynamic motion of both ethanol and water molecules and their desorption process on the permeated side, which facilitates the molecules transport through the membrane. It is worth noticing that the apparent activation energy of ethanol and water permeability, which was calculated from the Arrhenius plots (Fig. 3), has almost the same value for ethanol and water. The low apparent activation energy suggests that the ethanol and water crossover process involves only physical actions. The almost similar value of the activation energy, which is about 12 kJ mol^{-1} indicates that ethanol and water diffuse primarily through the water phase. This observation is in agreement with the reported results of Freger et al. [14]. Focusing on the water permeation activation energy, one can compare this to the activation energy of the conduction of protons through the membrane. It has been reported [15] that the latter has a value of about 10 kJ mol^{-1}, similar to the one measured in the present work for water permeation. This could imply that the mechanism by which water molecules move through the membrane pores is of the same nature as the one of protons' motion through the membrane.

As it has already been shown above, there is a maximum on both ethanol and water crossover rate versus the concentration, which is also appearing in Figs. 4 and 5. For example, in the case of water, at helium flow rate equal to 160 mL min^{-1}, for temperature equal to 60 °C and ethanol concentration 2.0 mol L^{-1} the crossover rate is 3.358 μmol cm^{-2} s^{-1} while at ethanol con-

centration 8.0 and 12.0 mol L^{-1} the crossover rate is 4.013 and 2.050 μmol cm^{-2} s^{-1}, respectively. For the temperature of 90 °C under the same conditions, the corresponding values are 6.53, 3.734 and 3.085 μmol cm^{-2} s^{-1}, respectively.

3.2. The effect of ethanol feed concentration

The effect of the concentration of ethanol aqueous solutions on water and ethanol crossover rates is shown in Figs. 4 and 5. As far as ethanol crossover is concerned, it can be clearly seen from Fig. 4(c and d) that there is a volcano behavior in the plot of ethanol crossover rate versus ethanol concentration. As shown in Fig. 5, a peak value for both ethanol and water crossover rate appears at $C_{EtOH} = 8.0$ and 2.0 mol L^{-1}, respectively, which increases with temperature. It is known that the ion exchange membrane swelling behavior depends on external solution concentration, which has a significant impact on the membrane's diffusion permeability [16]. It is reported that when different substances get into contact with the membrane material, a strong coupling effect can be observed for both solubility and diffusion [17]. In the present case, when the binary mixture of ethanol and water is brought in contact with Nafion® membrane, the coupling effect of solubility, swelling and flux between these two components is usually dependent on the concentration of ethanol in the mixture [23,24]. This volcano behavior could be related to the ethanol's solubility and Nafion® membrane's swelling state. Elliot et al. [18] have already reported that the macroscopic swelling degree of Nafion® membrane is produced to a much greater degree in the presence of ethanol, with a peak value in macroscopic swelling at 75% (v/v) ethanol. The other key factor, which should be considered, is that the ethanol diffusion coefficient is different at various ethanol concentrations [19].

In the case of water crossover shown in Fig. 4(a and b), it is clear that the behavior of water crossover as a function of ethanol concentration is not quite different from that of ethanol. Generally, permeability is directly related to solubility and diffusivity. For water the effective diffusion coefficient follows a smooth, monotonic increase with concentration [19–22].

3.3. The effect of helium flow rate F_{He}

The effect of helium flow rate at the cathode side on the crossover rate at different operation temperatures of the cell is shown in Fig. 6. It is obvious that the crossover rate of both ethanol and water increases as helium flow rate increases. In the present work, there is neither potential nor pressure difference between the anode and the cathode. Therefore, the main force for water and ethanol crossover is diffusion, which is caused by the existence of activity gradient between the two sides of Nafion® membrane. The increased crossover rate of ethanol and water can be attributed to a decreased activity in the gas side with the increase of helium flow rate. The activity of both water and ethanol at the cathode can be described by the following equation [13]:

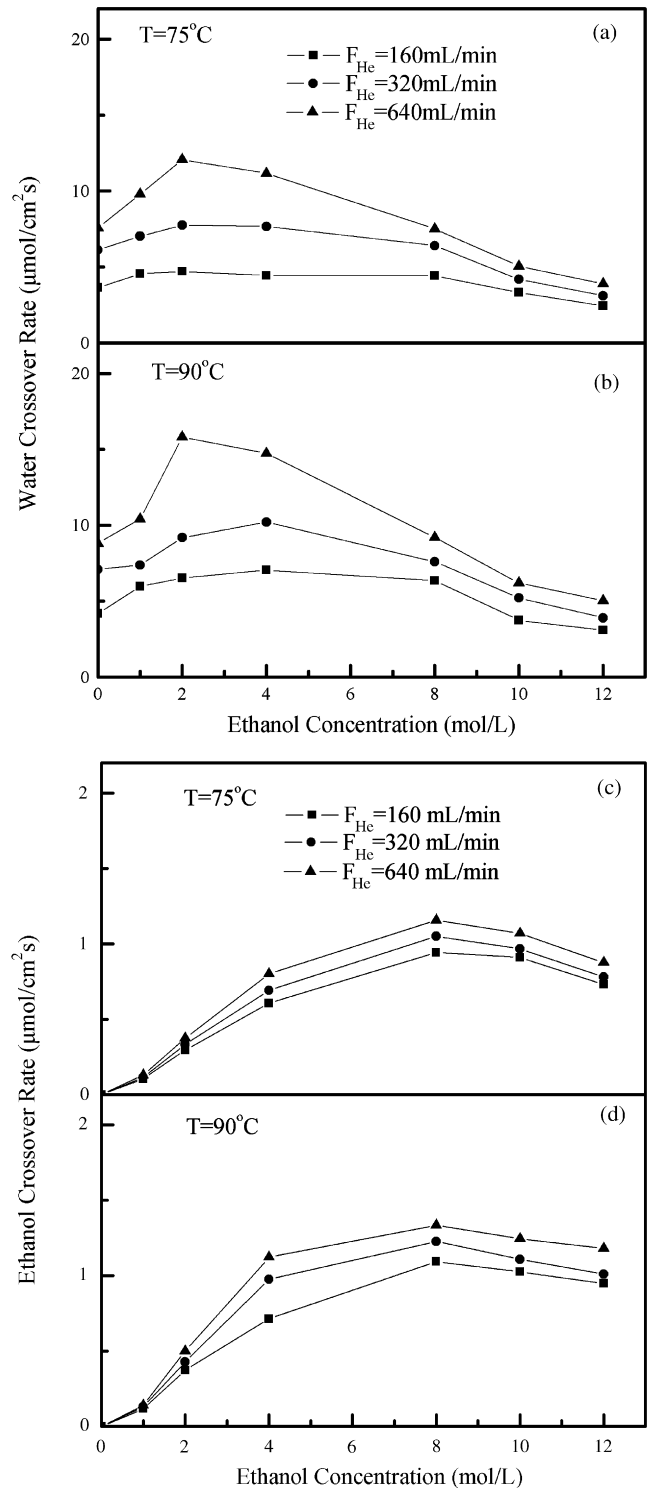$$a_i = \frac{V_i}{V_i + V_{He}} \frac{P}{P(T)}$$

Fig. 4. The effect of ethanol concentration at different flow rates (a) for the water and (b) for ethanol crossover rate. Cell operation temperature: 75 and 90 °C, anode liquid flow = 0.2 mL min^{-1}, $P_{total} = 1$ atm and electrode area = 4 cm^2.

where V_i and V_{He} denote the volumetric flow rates of i (water or ethanol) and helium, respectively, P the operation pressure of the cell and $P(T)$ is the saturation pressure of ethanol or water as a function of temperature.

It can be easily deduced from the above equation that as helium flow rate increases, the activity of both water and ethanol
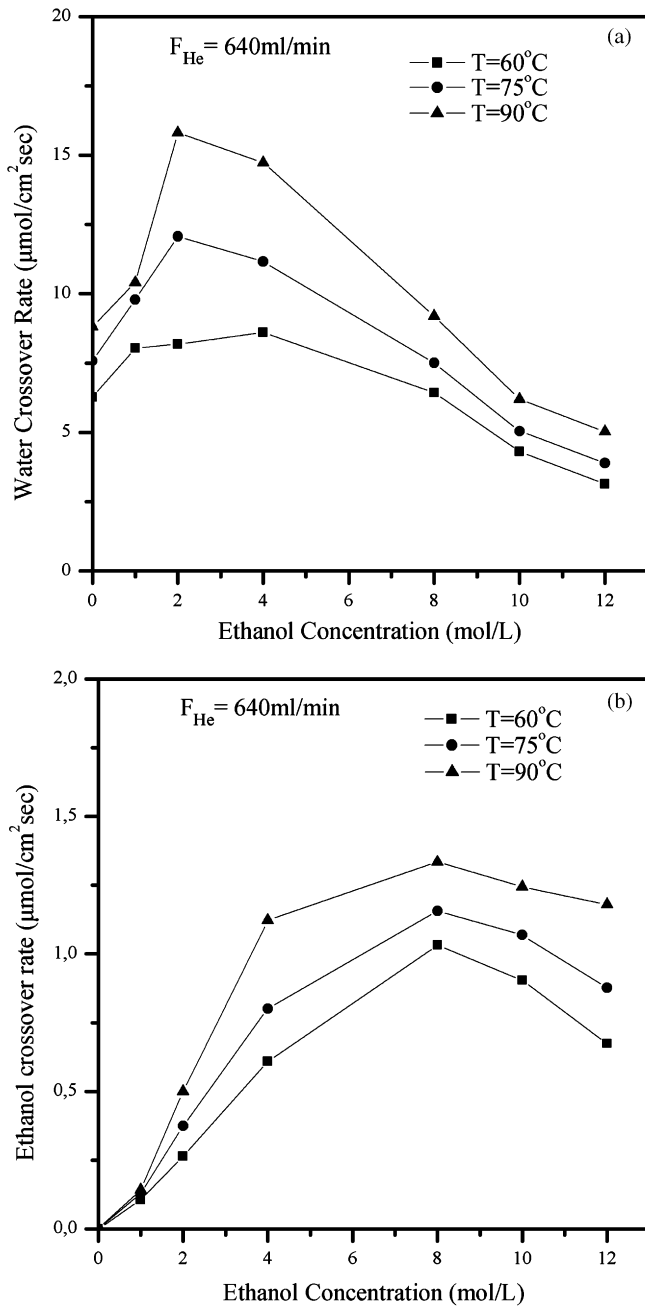
Fig. 5. The effect of ethanol concentration at different temperatures (a) for the water and (b) for ethanol crossover rate. Helium flow rate at the cathode = 640 mL min^{-1}, anode liquid flow = 0.2 mL min^{-1}, P_{total} = 1 atm and electrode area = 4.0 cm^2.

Fig. 6. The effect of helium flow rate at different operation temperatures (a) for water and (b) for ethanol crossover rate. Anode liquid flow = 0.2 mL min^{-1}, P_{total} = 1 atm and electrode area = 4.0 cm^2.

in the cathode decreases, leading to an increased activity gradient between the anode and the cathode, which consequently results in the increment of both ethanol and water crossover rates. At very high He flow rates, where the value of V_{He} is very big, the denominator in the above equation tends to infinity and leads to an almost zero activity of the permeated ethanol and water at the cathode side. Under these conditions, both ethanol and water permeation through the MEA will be considered that it is insensitive to the He flow rate. This can also be proved by Fig. 6, where ethanol and water crossover rates tend to reach a maximum value at higher He flow rates.
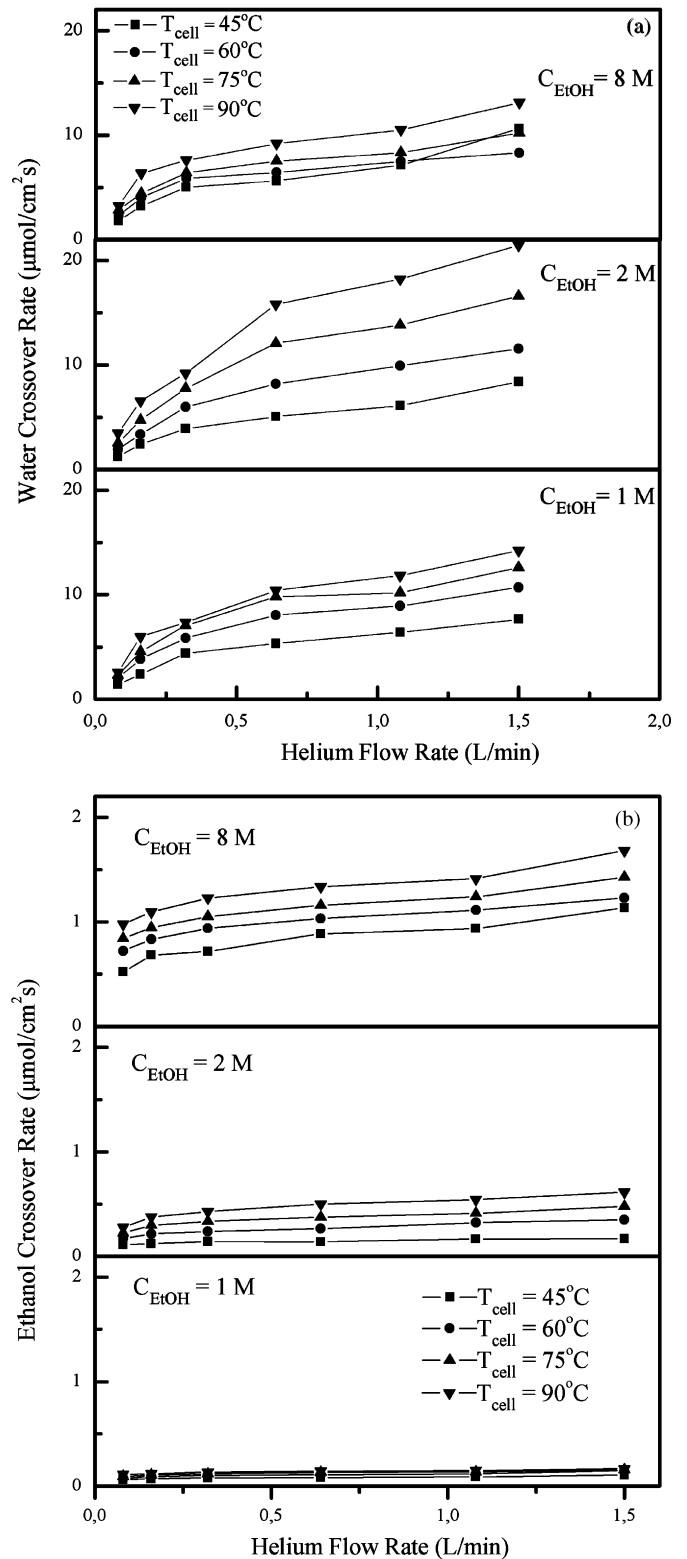
In the case of ethanol crossover, shown in Fig. 6(b), it is observed that ethanol crossover rate is one order of magnitude less than that of water presented in Fig. 6(a). Taking into account the similar activation energy for ethanol and water crossover, this

difference between their crossover rates is probably because of the fact that the sulphonic groups render some part of the aqueous phase in the solid polymer electrolyte (SPE) inaccessible to ethanol but still accessible to water. This is the result of the much stronger interaction between sulphonic groups with water than with ethanol [14]. Moreover, the larger molecule size of ethanol, compared to that of water, also contributes to the relatively small crossover rate of ethanol.

3.4. Nafion® membrane swelling behavior

In order to check whether the swelling behavior of Nafion® membrane is reversible or not, pure water crossover measurement was carried out twice. One was performed before any ethanol aqueous solution was supplied to the cell and the other was performed after all crossover measurements with different ethanol aqueous concentrations at different operation temperatures. The second measurement was performed after flushing water throughout the cell for at least 3 h in order to remove as much as possible from the ethanol residue, which was left in the membrane. Fig. 7 presents the comparison of the two different water crossover measurements results. It can be clearly seen from Fig. 7 that there is some difference between these two experimental results, especially in higher flow rates. This could be resulted from the partial loss of structural memory of Nafion® membrane related to the structural changes in the fluorocarbon matrix from the interaction of ethanol with the membrane [17,18].
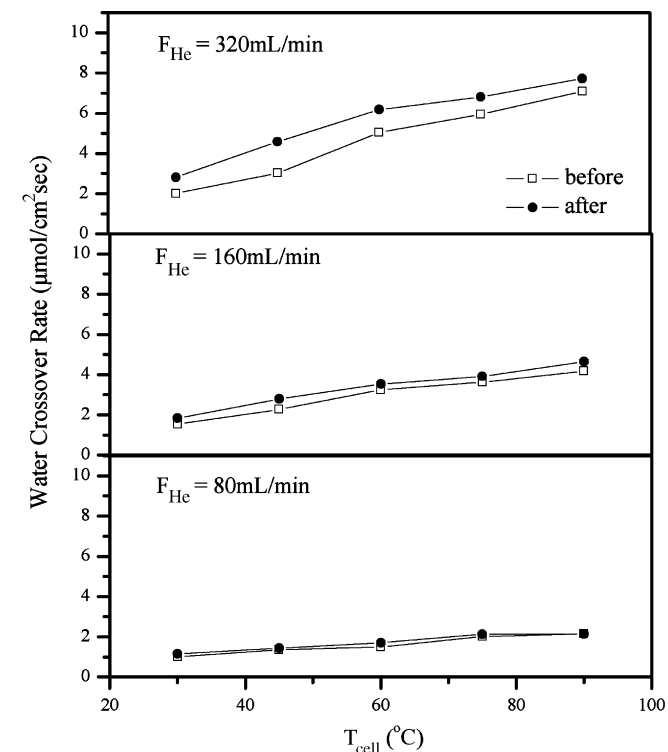

Fig. 7. Comparison of water crossover rate before and after crossover measurements.

4. Conclusion

Based on the systematical investigation of ethanol and water crossover in a wide range of operation conditions, it was found that, by increasing the gas carrier flow rate at the permeate side the permeation rate of both ethanol and water crossover was enhanced. The different dependence behavior of ethanol and water crossover rate on the ethanol concentration could be due to the different interaction of their molecules with Nafion® membrane in the case of ethanol and in the different interaction between the molecules of water and ethanol in the case of water. Ethanol crossover is one order of magnitude less than that of water, as a result of the different interaction of ethanol molecules with the Nafion® membrane and a bigger molecular size of ethanol.

The increment of temperature leads to the increment of both ethanol and water crossover rates. The almost similar activation energy for both ethanol and water, which is about $12 \, kJ \, mol^{-1}$, leads to the conclusion that under these operation conditions the main mechanism of crossover is diffusion through the membrane in the present investigated conditions.

References

[1] S.Q. Song, P. Tsiakaras, Appl. Catal. B 63 (2006) 187.
[2] S.Q. Song, W.J. Zhou, L.H. Jiang, G.Q. Sun, Q. Xin, V. Leontidis, S. Kontou, P. Tsiakaras, Int. J. Hydrogen Energy 30 (2005) 995.
[3] S. Song, W. Zhou, Z. Liang, R. Cai, G. Sun, Q. Xin, V. Stergiopoulos, P. Tsiakaras, Appl. Catal. B: Environ. 55 (2005) 65.
[4] S.Q. Song, Z.X. Liang, W.J. Zhou, G.Q. Sun, Q. Xin, V. Stergiopoulos, P. Tsiakaras, J. Power Sources 145 (2005) 495.
[5] S. Song, G. Wang, W. Zhou, X. Zhao, G. Sun, Q. Xin, S. Kontou, P. Tsiakaras, J. Power Sources 140 (2005) 103.
[6] J.T. Hinatsu, M. Mizuhata, H. Takenaka, J. Electrochem. Soc. 141 (1994) 1493.
[7] T.A. Zawodzinski, T.E. Springer, J. Danvey, R. Jestel, C. Lopez, J. Valerio, S. Gottesfeld, J. Electrochem. Soc. 140 (1993) 1041.
[8] T.A. Zawodzinski, M. Neeman, L.O. Sillerud, S. Gottesfeld, J. Phys. Chem. 95 (1991) 6040.
[9] T.A. Zawodzinski, C. Derouin, S. Radzinski, R.J. Sherman, V.T. Smith, T.E. Springer, S. Gottesfeld, J. Electrochem. Soc. 140 (1993) 7.
[10] T.E. Springer, T.A. Zawodzinski, G. Gottesfeld, J. Electrochem. Soc. 138 (1991) 2334.
[11] A.M. Affoune, A. Yamada, M. Umeda, J. Power Sources 148 (2005) 9.
[12] G. Andreadis, S. Song, P. Tsiakaras, J. Power Sources 157 (2006) 657.
[13] A.J. Motupally, J.W. Becker, Weidner, J. Electrochem. Soc. 147 (2000) 3171.
[14] V. Freger, E. Korin, J. Wisniak, E. Korngol, M. Ise, K.D. Kreuer, J. Membr. Sci. 160 (1999) 213.
[15] T.A. Zawodzinski, T.E. Springer, F. Uribe, S. Gottesfield, Solid State Ionics 60 (1993) 199.
[16] S.P. Nunes, K.V. Peinemann, Membrane Technology in the Chemical Industry, WILEY-VCH, Weinheim, 2001, 233.
[17] J. Hauser, G.A. Reinhard, F. Stumn, A. Heintz, Fluid Phase Equilib. 49 (1989) 195.
[18] J.A. Elliot, S. Hanna, A.M.S. Elliot, G.E. Cooley, Polymer 42 (2001) 2251.
[19] D. Rivin, C.E. Kedrick, P.W. Gibson, N.S. Schneider, Polymer 42 (2001) 623.
[20] R. Jiraratananon, A. Chavachai, R.Y.M. Huang, J. Membr. Sci. 199 (2002) 211.

[21] G.Q. Lu, F.Q. Liu, C.Y. Wang, Electrochem, Solid-State Lett. 8 (2005) A1.

[22] J.F. Van der Maelen Uria, C.A.R. Alvarez, Comp. Chem. 22 (1998) 225.

[23] S. Kato, K. Nagahama, H. Noritomi, H. Asai, J. Membr. Sci. 72 (1992) 31.

[24] V.M. Barragan, C. Ruiz-Bauza, J.P.G. Villaluenga, B. Seoane, J. Power Sources 130 (2004) 22.